Study of the control structure of a small wind turbine with permanent magnet synchronous generator

O. Carranza[1,2], E. Figueres[2], G. Garcerá[2], R. Ortega[1,2], C.L. Trujillo[2,3]

[1]Escuela Superior de Cómputo - Instituto Politécnico Nacional, Av. Juan de Dios Bátiz S/N, D. F., 07738, México.

[2]Departamento de Ingeniería Electrónica – UPV, Camino de Vera S/N, 7F, Valencia, 46022, España.

[3]Department of Electronic Engineering, Universidad Distrital Francisco José de Caldas. Carrera 7 N° 40-53 Piso 5, Bogotá, Colombia

ocarranzac@ipn.mx, efiguere@eln.upv.es, ggarcera@eln.upv.es, rortegag@ipn.mx, cltrujillo@udistrital.edu.co

Abstract- **This paper presents the analysis of the two control structures used in wind generation systems with permanent magnet synchronous generators, variable speed and fixed pitch, to determine which structure is most appropriate for implementation. These control structures are speed control and torque control. The analysis considers all the elements of wind power generation system, with greater emphasis on the model of the turbine where mechanical torque is considered as a system variable and not as in other studies where it is considered as internal disturbance in the system. The analysis is developed so that the control structure is independent of AC/DC converter that is used in the system. From the analysis is obtained that the speed control can be stable using classical control techniques because it is a nonminimum phase system and the torque control is unstable because it has poles and zeros in the right half plane, very low frequency and very close to each other, so it is very difficult to control using classical control theory. In the evaluation of the speed control structure, the AC/DC converter is Three-phase rectifier Boost in Discontinuous Conduction Mode with an input filter and a Peak Current Control and to avoid the need of mechanical sensors, a Linear Kalman Filter has been chosen to estimate the generator speed.**

INTRODUCTION

Wind Generation Systems (WGS) are currently taking a great interest in renewable energy systems [1]. This is mainly due to the high cost of fossil fuels and the need for clean energy sources. Although in the case of wind energy some places are not suitable for fully take advantage of this energy.

Currently wind energy can be used under various schemes, that is, primary source with storage systems provide energy in remote locations [2]; as primary energy source with conventional sources to inject energy into a grid; and as an energy source in microgrids schemes in distributed generation systems [3]. In small power wind generation systems ranging from *1kW* to *50kW*, permanent magnet synchronous generators (PMSGs) are preferred to other electrical machines like induction generators (IGs) [4]. PMSGs can work in grid isolated geographical zones and in a wide wind speed range, extracting a higher energy from the wind [4] than IGs. Due to the fact that both the output voltage and the frequency of a PMSG depend on the wind speed, An AC/DC converter and a DC/AC converter (inverter) are required for connecting the generator to the grid. The inverter is responsible for regulating active and reactive power, which is injected to the grid, and it controls the voltage of the DC-Link. There are basically two types of configurations of converters used when it has a PMSG, the first type is an uncontrolled rectifier and a DC/DC converter and the other type is a controlled rectifier.

The topology that uses the controlled rectifier and inverter, it is known as converter back-to-back.

One of the important points in wind power generation systems is to convert the most energy from wind power, seeking to achieve high levels of efficiency and quality of energy that is injected into the grid, which leads the implementation of different control strategies [5]-[6]. For the case under study, where the WGS uses a PMSG, the system operates at variable speed and fixed pitch; the control structures used are torque control and speed control.

Note that in both cases there is a torque control through the generator output current, only in the case of torque control is straightforward and in the case of speed control is an indirect torque control through an intermediate stage that controls the generator speed [7]. The torque control structure proposed in the SGE is shown in Fig. 1 and the speed control structure proposed in the SGE is shown in Fig. 2. The MPPT block represents the algorithm of the maximum power point tracking that provides the reference current (I_{ref}) in the control structure of torque (current) or provides the speed reference (ω_{ref}) in the structure of the speed control, which is outside the scope in this paper.
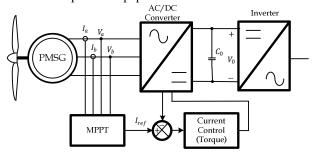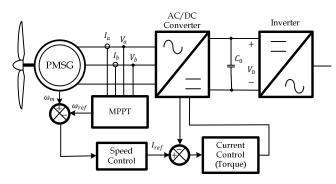

Fig. 1. Torque control structure in the SGE proposed.

Fig. 2. Speed control structure in the SGE proposed.

1900

This paper is focused on the analysis both speed and torque control structures and design of the speed control loop of the system, which allows to have a stable system with a speed control structure. The analysis is developed to consider all the variables of the system, mainly the mechanical torque, because most of the systems, it is considered an internal disturbance of the system to simplify the system. The analysis of the control structure is independent of the type of AD/DC converter which is used in the WGS, as well as the current control used. To test the proper selection of the control structure, it is used three-phase boost rectifier working in DCM with LCL input filter as a AC/DC converter and a peak current mode control, both are described in [8].

Table I shows the values of the parameters of the wind generation system.

WIND TURBINE

A. Wind Turbine Model

The mechanical behavior of the wind turbine follows (1)

$$J\frac{d\omega_m}{dt} + B\omega_m = T_m - T_e \tag{1}$$

where J is inertia coefficient, B is the friction coefficient, ω_m is the turbine rotational speed, T_m is the turbine mechanical torque and T_e is the electrical torque applied to the PMSG rotor.

The mechanical power generated by the wind turbine (P_m) and T_m are expressed by equations (2) and (3), respectively.

$$P_m = \frac{1}{2}\rho\pi r^2 C_p(\lambda)V_\omega^3 \tag{2}$$

$$T_m = \frac{1}{2}\rho\pi r^3 C_t(\lambda)V_\omega^2 \tag{3}$$

Table I. Characteristics of the WGS

Characteristics	Values
Output power of the generator (P_o)	2 kW
Output voltage range of the generator ($V_{ab} = V_{bc} = V_{ca}$)	$104 - 416\ Vrms$
Constant of the electromotive force (K_{fem})	$0.9022\ Vpeak/rad/s$
Number of poles (n_p)	12
Speed range of the generator (n_m)	$150 - 600\ rpm$
Angular mechanical frequency range of the generator (ω_m).	$15.7 - 62.83\ rad/s$
Angular electrical frequency range of the generator (ω_e)	$94.2 - 376.98\ rad/s$
Inductance of one phase of the generator ($L_{ga} = L_{gb} = L_{gc}$)	$25\ mH$
Resistance of one phase of the generator ($R_{Lga} = R_{Lgb} = R_{Lgc}$)	$5\ \Omega$
Wind turbine coefficients	$a = 0.043, b = 0.108, c = 0.146,$ $d = 0.0605,\ e = 0.0104, f = 0.0006$
Wind turbine ratio (r)	$1.525\ m$
Inertia Coefficient of the system (J)	$0.5\ kg\ m/\ s2$
Density of wind (ρ)	$1.08\ kg/m3$
DC link Capacitance (C_0)	$2\ mF$
DC link voltage (V_0)	$650\ V$
Sampling time (T_s)	$10\ \mu s$

where ρ is the density of the air, r is the wind turbine rotor radius, V_ω is the wind speed, $C_p(\lambda)$ is the power coefficient, it is expressed by (4), $C_t(\lambda)$ is the torque coefficient, it is expressed by (5). Both coefficients depend on the tip-speed-ratio parameter(λ), and it is expressed by (6).

$$C_p(\lambda) = a + b\lambda + c\lambda^2 + d\lambda^3 + e\lambda^4 + f\lambda^5 \tag{4}$$

$$C_t(\lambda) = \frac{C_p(\lambda)}{\lambda} \tag{5}$$

$$\lambda = \frac{rW_m}{V_\omega} \tag{6}$$

B. Permanent Magnet Synchronous Generators Model

The equivalent circuit of the permanent magnet synchronous generator [7] is shown in Fig. 3. Where $L_{ga} = L_{gb} = L_{gc}$ are the inductances of one phase, $R_{Lga} = R_{Lgb} = R_{Lgc}$ are the resistance in series of one phase, V_a, V_b and V_c are the generator instantaneous output voltages and e_a, e_b and e_c are the electromotive forces.

The electric equations of the PMSG are described by (7).

$$\begin{bmatrix} V_a \\ V_b \\ V_c \end{bmatrix} = -R_g\begin{bmatrix} i_a \\ i_b \\ i_c \end{bmatrix} - L_g\frac{d}{dt}\begin{bmatrix} i_a \\ i_b \\ i_c \end{bmatrix} + \begin{bmatrix} e_a \\ e_b \\ e_c \end{bmatrix} \tag{7}$$

Analyzing the behavior of the PMSG, it is obtained that the electromotive torque (T_e) is determined by (8)

$$T_e = \frac{3K_{emf}I_g}{\sqrt{2}} \tag{8}$$

where K_{emf} is the constant of the electromotive force and I_g is the generator phase rms current.

MODELLING WIND GENERATION SYSTEM

The main goal in wind power generation system is to extract the greatest amount of wind energy and transform it in electric energy. This is achieved with an appropriate algorithm of the Maximum Power Point Tracking (MPPT) and adequate control structure that allows the system to be stable in the range of operation. Whereas the mechanical power of the turbine (P_{mec}) is equal to the electric power generator (P_{out}), having into account the electrical losses of the generator. The generator output power is expressed by

$$P_{mec} = P_{out} = T_e\omega_m - R_{Lga}I_g \tag{9}$$
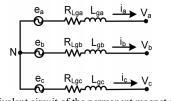
Applying (8) in (9), it is obtained:

Fig. 3. Equivalent circuit of the permanent magnet synchronous generator.

$$P_{out} = \frac{3K_{fem}}{\sqrt{2}} I_g \omega_m - R_{Lga} I_g \qquad (10)$$

Because the power function is not linear, a linear model of P_{out} may be obtained by applying a first order Taylor series around the operation point. This linear model allows a small-signal analysis to determine which control system is most suitable. Developing, it is obtained

$$\hat{P}_{out} = \hat{\omega}_m \frac{3K_{fem}}{\sqrt{2}} I_g + \hat{\imath}_g \left(\frac{3K_{fem}}{\sqrt{2}} W_m - R_{Lga} I_g \right) \qquad (11)$$

From (11), the analysis can be performed to select which of the two control structures is the most appropriate for this WGS. By (11), it is shown that the generator output power has a dependence of both the generator current and the generator speed.

To analyze the two control structures in the WPGS, it is necessary obtain the dependence of the power function of a single variable. If the control structure is analyzed through the torque, it is necessary obtain the relationship between the generator output power and generator torque $(\hat{P}_{out}/\hat{T}_e)$ or the relationship between the generator output power and generator current$(\hat{P}_{out}/\hat{\imath}_g)$, because the generator torque has a direct relationship with the current generator as shown in (9). If the control structure is analyzed through the generator speed, it is necessary obtain the relationship between the generator output power and generator speed $(\hat{P}_{out}/\hat{\omega}_m)$.

To analyze the torque control structure, it is necessary to obtain the $\hat{P}_{out}/\hat{\imath}_g$. Starting from equation (11), it is obtained (12). In (12) is observed that $\hat{P}_{out}/\hat{\imath}_g$ depends on the $\hat{\omega}_m/\hat{\imath}_g$.

$$\frac{\hat{P}_{out}}{\hat{\imath}_g} = \frac{\hat{\omega}_m}{\hat{\imath}_g} \frac{3K_{fem}}{\sqrt{2}} I_g + \frac{3K_{fem}}{\sqrt{2}} W_m - 2R_{Lga} I_g \qquad (12)$$

To analyze the speed control structure, it is necessary to obtain the $\hat{P}_{out}/\hat{\omega}_m$. Starting from equation (11), it is obtained (13). It is also necessary to implementing a speed control loop to complete the control structure. In (13) is observed that $\hat{P}_{out}/\hat{\imath}_g$ depends on the $\hat{\imath}_g/\hat{\omega}_m$.

$$\frac{\hat{P}_{out}}{\hat{\omega}_m} = \frac{3K_{fem}}{\sqrt{2}} I_g + \frac{\hat{\imath}_g}{\hat{\omega}_m} \left(\frac{3K_{fem}}{\sqrt{2}} W_m - 2R_{Lga} I_g \right) \qquad (13)$$

Starting from equation (1), it is obtained (14).

$$\omega_m = \frac{1}{Js} (T_m - T_e) \qquad (14)$$

T_m is normally considered an internal disturbance in the system. However, T_m strongly depends on both the speed of the PMSG, ω_m, and the wind speed, v_ω, as it is shown in (3)-(5). T_e depends on the I_g as shown in (8).Therefore, in this paper include T_m, so considering all the variables involved in the system, which allows a complete analysis of the system.

Applying (6), (4) and (5) in (3), it is obtained:

$$T_m = \frac{1}{2}\rho\pi r^3 \left(\frac{av_\omega}{r\omega_m} + b + \frac{cr\omega_m}{v_\omega} + \frac{dr^2\omega_m^2}{v_\omega^2} + e\frac{r^3\omega_m^3}{v_\omega^3} + f\frac{r^4\omega_m^3}{v_\omega^4} \right) v_\omega{}^2 \qquad (15)$$

Because of the T_m is not linear, a linear model of T_m may be obtained by applying a first order Taylor series around the operation point. Note that one of the inputs of the resulting linear model is the wind speed, which is considered as an external disturbance, and the other one is the inherent feedback of the generator speed. Developing, and as the wind speed is an external disturbance, $\hat{v}_\omega = 0$ is considered to analyze the stability of the speed control loop. The small-signal term of T_m is expressed by (16).

$$\hat{T}_m|_{\hat{v}_\omega=0} = \frac{1}{2}\rho\pi r^3 \left(-\frac{aV_\omega^3}{rW_m^2} + crV_\omega + 2dr^2W_m + \frac{3er^3W_m^2}{V_\omega} + \frac{4fr^4W_m^3}{V_\omega^2} \right) \hat{\omega}_m \qquad (16)$$

PMSG speed is expressed by (17).

$$\hat{\omega}_m = \frac{1}{Js} \left(\hat{T}_m|_{\hat{v}_\omega=0} - \hat{T}_e(i_g) \right) \qquad (17)$$

From (16)-(17), it is obtained the relationship between the PMSG speed and generator current, it is expressed by

$$G_{\omega g}(s) = \frac{\hat{\omega}_m}{\hat{\imath}_g} = -\frac{3K_{fem}}{\sqrt{2}\left[Js - \frac{1}{2}\rho\pi r^3 c_1 \right]}$$
$$c_1 = \left(-\frac{aV_\omega^3}{rW_m^2} + crV_\omega + 2dr^2W_m + \frac{3er^3W_m^2}{V_\omega} + \frac{4fr^4W_m^3}{V_\omega^2} \right) \qquad (18)$$

TORQUE CONTROL VS SPEED CONTROL

In order to determine which control structure is the most suitable for use in the proposed wind generation system. It is necessary to obtain $\hat{P}_{out}/\hat{\imath}_g$ to analyze the torque control and $\hat{P}_{out}/\hat{\omega}_m$ to analyze the speed control.

Analyzing the torque control structure, it is substituted (18) in (12), obtaining the transfer function from the generator current to generator output power, it is expressed by

$$\frac{\hat{P}_{out}}{\hat{\imath}_g} = \frac{-9K_{fem}{}^2 I_g + \left(\frac{3K_{fem}}{\sqrt{2}} W_m - 2R_{Lga} I_g \right)[2Js - \rho\pi r^3 c_1]}{[2Js - \rho\pi r^3 c_1]}$$
$$c_1 = \left(-\frac{aV_\omega^3}{rW_m^2} + crV_\omega + 2dr^2W_m + \frac{3er^3W_m^2}{V_\omega} + \frac{4fr^4W_m^3}{V_\omega^2} \right) \qquad (19)$$

Fig. 4 shows Bode diagrams of the transfer function from $\hat{P}_{out}/\hat{\imath}_g$ to $V_\omega = 10\ m/s$, as a function of λ. Fig. 4 shows that $\hat{P}_{out}/\hat{\imath}_g$ is unstable for λ values greater than 3.

This is corroborated in Fig. 5, which shows the location of the roots of $\hat{P}_{out}/\hat{\imath}_g$, for λ values between 4 and 7; note that the poles and zeros are in the right half plane at very low frequency and very close to each other for different operating points. This allows to establish that torque control structure is very complicated to implement using classical control theory. Analyzing the speed control structure, it is substituted (18) in (13), obtaining the transfer function from the generator speed to generator output power, it is expressed by
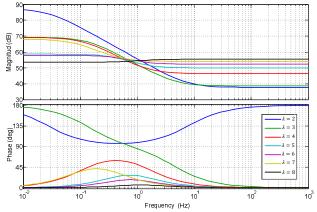
Fig. 4. Bode diagrams of the transfer function from the $\hat{P}_{out}/\hat{\imath}_g$ to $V_\omega = 10$ m/s, as a function of λ.
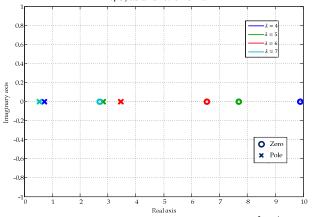

Fig. 5. Location of the roots of the transfer function from the $\hat{P}_{out}/\hat{\imath}_g$ to $V_\omega = 10$ m/s, as a function of λ.

$$\frac{\hat{P}_{out}}{\hat{\omega}_m} = \frac{3K_{fem}}{\sqrt{2}}I_g - \left(W_m - \frac{2\sqrt{2}R_{Lga}I_g}{3K_{fem}}\right)\left[Js - \frac{1}{2}\rho\pi r^3 c_1\right]$$
$$c_1 = \left(-\frac{aV_\omega^3}{rW_m^2} + crV_\omega + 2dr^2W_m + \frac{3er^3W_m^2}{V_\omega} + \frac{4fr^4W_m^3}{V_\omega^2}\right) \quad (20)$$

Fig. 6 shows Bode diagrams of the transfer function from $\hat{P}_{out}/\hat{\omega}_m$ to $V_\omega = 10\ m/s$, as a function of λ. Fig. 6 shows that $\hat{P}_{out}/\hat{\omega}_m$ is non-minimum phase system, because contains zeros in the right half plane, for various values of λ. This allows to establish that speed control structure can be implemented using classical control techniques.

IMPLEMENTATION OF THE STRUCTURE SPEED CONTROL

A. AC/DC Converter and Current Control Loop
The AC/DC converter used is a Three-Phase Boost Rectifier operating in Discontinuous Conduction Mode (DCM) with Peak Current Mode Control (PCC), this was presented and analyzed in [8]. The Boost Rectifier operating in DCM achieves a Total Harmonics Distortion (THD$_i$) of the generator currents, much lower than that achieved by the same topology operating in Continuous Conduction Mode (CCM), improving the power factor of the generator. In the current paper it is only presented the most relevant issues to assess the speed control structure in the proposed wind generation system.
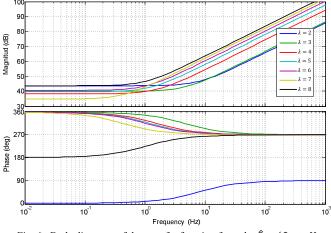

Fig. 6. Bode diagrams of the transfer function from the $\hat{P}_{out}/\hat{\omega}_m$ to $V_\omega = 10\ m/s$, as a function of λ.

$G_{id}(s) = \hat{\imath}_L(s)/\hat{d}(s)$ is the transfer function from the duty cycle to the equivalent boost inductor current, expressed by (21).

$$G_{id}(s) = \frac{\hat{\imath}_L(s)}{\hat{d}(s)} = \frac{-(s^2C_iL_g + sC_iR_g + 1)(K_i + K_o)}{s^3B_3 + s^2B_2 + sB_1 + B_0}$$

$$\begin{aligned}
B_3 &= C_iL_gL(g_i + g_o + g_f) \\
B_2 &= C_i\left[L_g + (g_i + g_o + g_f)\left(LR_{L_g} + L_gR_L\right)\right] \\
B_1 &= \left[C_iR_{L_g} + (g_i + g_o + g_f)\left(L_g + L + C_iR_LR_{L_g}\right)\right] \\
B_0 &= (g_i + g_o + g_f)\left(R_{L_g} + R_L\right) + 1
\end{aligned} \quad (21)$$

where the values of the parameters of the PWM switch small-signal model in DCM [9] are shown in (22).

$$g_i = \frac{D^2}{2Lf_s} \qquad g_o = \frac{2LP_o^2f_s}{D^2V_i^2V_o^2} \qquad g_f = \frac{2P_o}{V_iV_o}$$
$$K_i = -\frac{DV_i}{Lf_s} \qquad K_o = -\frac{2P_o}{DV_o} \quad (22)$$

In (21) and (22) it is considered: $L_g = 2L_{ga}$, $R_{Lg} = 2R_{Lga}$, $L = 2L_a$, $R_L = 2R_{La}$ and $C_i = 3C_{f1}/2$. D is the duty cycle of the boost active switch. V_i is the average value of the Boost DC-DC converter input voltage. The boost rectifier output voltage, V_o, is regulated by the grid connected inverter to a constant value of *650V*. P_o is the output power at the operating point, which is limited to the maximum value allowed by the PMSG. Fig. 7 shows the block diagram of the current loop with PCC [10]. The reference for the current loop, I_{ref}, is provided by the controller of the speed control loop. The loop gain of the current loop, $T_i(s)$, is determined by (23). $R_i = 0.015\ \Omega$ is the current sense gain, F_M is the PWM modulator gain, and $H_e(s)$ is the sampling gain [10].
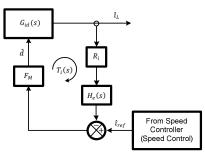
$$T_i(s) = G_{id}(s)H_e(s)R_iF_M \quad (23)$$

Fig. 7. Peak Current-Mode Control Loop.

The closed loop gain of the current loop is given by

$$G_{ic}(s) = \frac{\hat{i}_L(s)}{\hat{i}_{ref}(s)} = \frac{G_{id}(s)F_M}{1 + T_i(s)} \tag{24}$$

As the PMSG torque depends on the generator currents, it is important to know the relationship between the generator current and the equivalent boost inductor current, following (25).

$$\frac{\hat{i}_g(s)}{\hat{i}_L(s)} = \frac{1}{s^2 C_i L_g + s C_i R_{Lg} + 1} \tag{25}$$

B. Speed Control Loop

Once set the AC / DC converter used in the WGS, it is performed small-signal analysis of the system around the operating point and it is developed the speed loop for the system is stable to variations in generator speed.

This analysis of the dynamics of the turbine expressed by (14), considering the mechanical torque developed in (16) and the electric torque, depends on the generator current expressed, the current control loop, which includes Boost-phase rectifier and input filter represented in (24) and (25), respectively, Fig. 8 shows the block diagram of the speed control loop.

Where $K = 1$ is the speed sensing gain, G_ω is the transfer function of a simple proportional-integral controller and ω_{ref} is the reference speed loop, which is provided by a search algorithm for maximum power point, which is outside the scope of this paper.

To analyze the response of the system, wind speed is considered a disturbance input of the system, which provides that $\hat{v}_\omega = 0$, so that the relationship between speed generator and current generator is expressed by (18), also the current loop is reduced to the expressed in (24).
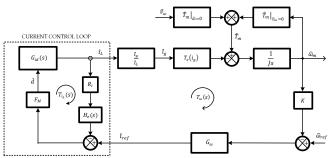

Fig. 8. Block diagram of the speed control loop

The loop gain of the speed loop, $T_\omega(s)$, is determined by (26).

$$T_\omega(s) = G_{ic}(s) G_{\omega g}(s) \frac{\hat{i}_g(s)}{\hat{i}_L(s)} K G_\omega(s) \tag{26}$$

The chosen gains for the PI speed controller, G_ω, are: $K_p = -0.05777$ and $K_i = -0.0187752 \ rad/s$. Fig. 9 shows the Bode diagrams of T_ω with the chosen controller.

C. Speed estimator

To obtain the feedback signal for the speed control loop, it is possible to mount speed sensors on the shafts of the PMSG (resolvers, encoders or Hall-effect sensors). However, the use of these sensors increases the complexity, weight and cost of PMSG. As both the voltages and frequency of the generator depend on its speed, the PMSG speed can be estimated starting from the measurement of the electrical quantities, eliminating the need for mechanical sensors. The problem is that the measured signals contain low frequency harmonics of the fundamental frequency of the generator, as well as switching frequency components due to the boost rectifier.

These issues have been studied in [11], concluding that the use of a Linear Kalman Filter (LKF) is a good compromise among dynamical response, static performance and complexity of implementation. In this case sensors are used to measure the generator output voltages in order to apply the LKF speed estimation. The main equations of the LKF used in this work are expressed by (27). The meaning of each variable of (27) in explained in [12].

$$\begin{aligned}
\varepsilon(k) &= V_\beta(k) \cos\theta(k) - V_\alpha(k) \sin\theta(k) \\
\theta(k+1) &= \theta(k) + T_s \omega_e(k) + K_{s1}\varepsilon(k) \\
\omega_e(k+1) &= \omega_e(k) + \dot{\rho}(k) + K_{s2}\varepsilon(k) \\
\dot{\rho}(k+1) &= \dot{\rho}(k) + K_{s3}\varepsilon(k)
\end{aligned} \tag{27}$$

The chosen values of the LKF parameters are: $\delta = 5 \times 10^6$, $K_{s1} = 0.0032896$, $K_{s2} = 0.54221$ and $K_{s3} = 0.00044647$. It is worth pointing out that the LKF gains are independent of the PMSG parameters and could be used with a different generator. Another advantage of the LKF speed estimator is that the only measurement needed is that of the output voltages of the PMSG, reducing the cost of the sensors in the system.
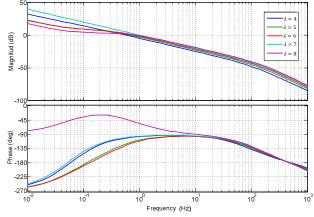

Fig. 9. Bode diagram of the speed loop gain, at a wind speed of $6 \ m/s$.

The performance of the proposed WECS has been evaluated by means of PSIM 7.0.5 software [11]. The system includes Boost rectifier in DCM with input filter and control PCC, the wind turbine model, the sensing speed by a speed estimator and the speed loop through the controller designed.

In order to evaluate whether the speed control structure is adequate in the WGS, in the reference speed are applied steps to observe the behavior of the WGS, with constant wind speed. The steps $(\Delta\omega_{ref})$ are 20 rpm, the update time (Δt) of the reference is 10s and the wind speed is 10 m/s. The reference speed starts at 150 rpm, however, the WGS is limited to a maximum reference speed, according to the behavior of the turbine, it is 530 rpm at 10 m/s,. Fig. 10 shows the behavior of the speed loop to steps in the speed reference at a constant wind speed of 10 m/s. It is observed that the speed loop properly follows the reference value. Figures also show the behavior of the electric torque and the PMSG output power. It is observed that the speed loop properly follows the reference value in all case.

Fig. 11 shows in detail the speed loop response to steps in the reference speed, which is observed as for the speed loop always follow the setpoint established by the reference speed, regardless of wind speed and whether the reference speed increase or decrease, thereby demonstrating the speed control structure is adequate in the wind generation system.

CONCLUSION

In the study of the control structures in wind power generation system was concluded that the speed control is best suited for implementation because it is a nonminimum phase system, which can be controlled by classical control theory, compared with the control of torque, which has poles and zeros in the right half plane, very low frequency and very close to each other, so it is very difficult to control using classical control theory. The study considered all the elements of WGS, taking great care of the turbine model, which considers the mechanical torque as a system variable and not as a perturbation internal system, idea used in other studies.

Furthermore the analysis of the control structure is
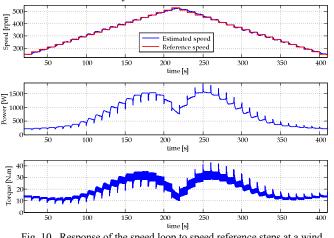

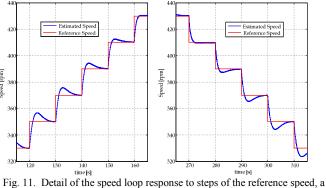Fig. 10. Response of the speed loop to speed reference steps at a wind speed of 10 m/s.

Fig. 11. Detail of the speed loop response to steps of the reference speed, a wind speed of 10 m/s

developed to be independent of the converters used on the system. The implementation of WGS for checking that the control structure is the most appropriate speed for this system, let to observe how the speed loop response to variations in the reference speed and how it stabilizes. In the implementation of the control structure is used a Three-phase rectifier Boost in DCM with an input filter and a PCC.

REFERENCES

[1] H. Li and Z. Chen, "*Overview of different wind generator systems and their comparisons*", IET Renewable Power Generation, Vol. 2, No. 2, pp. 123-138, June 2008.

[2] Patrick J. Luickx, Erik D. Delarue, William D. D'haeseleer, "Considerations on the backup of wind power: Operational backup", Applied Energy 85 (9), pp. 787-799, September 2008.

[3] C.L. Trujillo, D. Velasco, E. Figueres, G. Garcerá, "Analysis of active islanding detection methods for grid-connected microinverters for renewable energy processing", Applied Energy, 87 (11), pp. 3591-3605, November 2010.

[4] Jamal A. Baroudi, Venkata Dinavahi, Andrew M. Knight, "A review of power converter topologies for wind generators" Renewable Energy 32, pp. 2369-2385, 2007.

[5] E. Bossanyi, "The Design of closed loop controllers for wind turbines", Wind Energy, Vol. 3 No. 3, pp. 149-163, Sep 2000.

[6] F. D. Bianchi, H. De Battista, R. J. Mantz, "Wind Turbine Control Systems", Germany, Springer, 2007.

[7] Yin Ming, Li Gengyin, Zhou Ming, Zhao Chengyong, "Modeling of the Wind Turbine with a Permanent Magnet Synchronous Generator for Integration", IEEE Power Engineering Society General Meeting, 2007, 24-28 June 2007 pp. 1–6.

[8] O. Carranza, E. Figueres, G. Garcera, L. G. Gonzalez, F. Gonzalez-Espin, "Peak Current Mode Control of a Boost Rectifier with Low Distortion of the Input Current for Wind Power Systems based on Permanent Magnet Synchronous Generators", *13th European Conference on Power Electronics and Applications, EPE '09.* 8-10 Sept. 2009 pp. 1-10

[9] V. Vorperian, "Simplified analysis of PWM converters using model of PWM switch I and II" IEEE Trans. on Aerospace and Electronic Systems, vol. 26 (3), pp. 490-505, may 1990.

[10] R. B. Ridley, "A new, continuous-time model for current-mode control (power convertors)", IEEE Trans. on Power Electronics, vol. 6, no. 2, pp. 271-280, April 1991.

[11] PSIM 7.0 User´s Guide (2006), Powersim Inc., March 2006.

[12] O. Carranza, E. Figueres, G. Garcera, C. L. Trujillo, D. Velasco, "Comparison of Speed Estimators Applied to Wind Generation Systems with Noisy Measurement Signals", ISIE 2010 IEEE International Symposium on Industrial, 4-7 July 2010, pp. 3317-3322.